SAND2022-0020J

Observing and Modeling the Effects of Production Infrastructure in Electromagnetic Surveys

Chester J. Weiss[1,2], G. Didem Beskardes[1], Kris MacLennan[3], Michael J. Wilt[4], Evan Schankee Um[4] and Don C. Lawton[5]

1. Geophysics Department, Sandia National Laboratories, Albuquerque, NM, USA, cjweiss@sandia.gov and gdbeska@sandia.gov
2. Earth and Planetary Sciences Department, University of New Mexico, Albuquerque, NM USA, cjweiss@unm.edu
3. Energy & Environmental Research Center, University of North Dakota, Grand Forks, ND, USA, kmaclennan@undeerc.org
4. Earth and Environmental Sciences, Lawrence Berkeley National Laboratory, Berkeley, CA, USA, mwilt@lbl.gov and esum@lbl.gov
5. Department of Geoscience University of Calgary; Director, Containment and Monitoring Institute (CaMI), Calgary AB, Canada, lawton@ucalgary.ca

Abstract

Electromagnetic methods are among the original techniques for subsurface characterization in exploration geophysics because of their particular sensitivity to Earth electrical conductivity, physical property of rocks distinct yet complementary to density, magnetization and strength. However, this unique ability also makes them sensitive to metallic artifacts – infrastructure such a pipes, cables and other forms of cultural clutter – whose electromagnetic footprint often far exceeds their diminutive stature when compared to that of bulk rock itself. In the hunt for buried treasure or unexploded ordnance this is an advantage; in the long-term monitoring of mature oil fields after decades of production, it is quite troublesome indeed. Here we consider the latter through the lens of an evolving energy industry landscape where the traditional methods of electromagnetic characterization for the exploration geophysicist are applied toward emergent problems in well-casing integrity, carbon capture and storage, and overall situational awareness in oilfield. We introduce case studies from these exemplars, showing how signals from metallic artifacts can dominate those from the target itself, and impose significant burdens on the requisite simulation complexity. We also show how recent advances in numerical methods mitigate the computational explosivity of infrastructure modeling, providing feasible and real-time analysis tools for the desk-top geophysicist. Lastly, we demonstrate through comparison of field data and simulation results that incorporation of infrastructure into the analysis of such geophysical data is - in a growing number of cases - a requisite but now manageable step.

Introduction

Estimates of electrical properties inferred by direct current (DC) resistivity and electromagnetic (EM) surveys have a long history of providing useful constraints on both the geology and hydrogeophysical state of the subsurface. Recently, their utility in natural resource exploration and management has been extended to monitoring the state of health of anthropogenic infrastructure itself, most notably in the rapid and non-invasive characterization of cased wellbores to detect regions compromised by chemical or mechanical defects after placement (MacLennan et al., 2018; Um et al., 2018; Wilt et al., 2018; Wilt et al., 2020). Such applications of DC and EM methods are attractive because they can, in principle, avoid costly interruptions to production that results from deployment of downhole logging instruments in situations where defects are suspected. The physical basis for their success is the fact that such defects alter the imposed electric current pathways – either through changes in electrical conductivity, or in extreme instances, abrupt discontinuities – which consequently perturb any measurements of electric and/or magnetic fields taken thereafter. Regardless of the survey objectives, understanding EM data requires understanding where the current goes, and the dominant factor affecting where it goes when the survey is located in a region rich with anthropogenic "clutter" (**Figure 1**) is the clutter itself (Fitterman et al., 1990). This presents a problem. In extreme cases, signals may be completely masked by the infrastructure response and any interpretive "rules of thumb" that neglect the mutual interaction (both galvanic and inductive) between artifacts are of limited help.

Modeling multiscale conductive infrastructure is a longstanding problem in both DC resistivity and EM research. The main challenge is to explicitly discretize the spatial scales of highly-conductive infrastructure in the computational mesh, such as kilometers-long wells with small radii or meters-wide storage tanks with thin metallic walls, which subsequently results in extensive mesh refinement and therefore computationally demanding or even prohibitively costly simulations. The early literature is based dominantly on the approximate analytical and integral equation methods. Wait (1972) and Wait and Hill (1973) calculated the EM responses of an infinite line conductor and a vertical cylinder of finite length in a homogeneous half-space, respectively. Later, Qian and Boerner (1995) formulated an integral equation to study the EM response of bending line conductors in a layered earth. Several authors also focused on the effects of infrastructure on the DC responses (e.g., Wait, 1983; Holladay and West, 1984). Moreover, another integral equation approach called the method of moments (MoM) has been applied to simulate the EM response of metallic infrastructure where the conductive objects are deconstructed as a series of smaller segments and treated as an approximate sum of electric dipole sources (Swidinsky et al., 2013). Several authors applied MoM to various infrastructure scenarios including a single well in a half-space where it is considered as a grounded electrode for reservoir monitoring (Tang et al., 2015), vertical and tilted wells in a layered earth (Kohnke et al., 2017), multiple interacting wells (Patzer et al., 2017), bending horizontal casing or pipeline systems (Orujov et al., 2020).

In addition, parallelization of the computations (e.g., Commer et al., 2015; Um et al., 2015) and simplifying the geometry of steel-cased wells (Haber et al., 2016) have been considered to deal with the high computational cost resulting from fine-scale meshes. Cylindrical coordinates for the finite element method and the finite volume method have been also considered to study the DC and EM responses of vertical steel-cased wells (Cuevas and Pezzoli, 2018; Heagy and Oldenburg, 2019a,b). In the DC limit, various approaches have been proposed to model the electric response of steel-cased wells such as the conductive cell model (Rucker et al., 2010), the complete electrode model (Rücker and Günther, 2011), and the shunt electrode model (Zhang et al., 1995; Wang et al., 1999; Ronczka et al., 2015). Another approach is the equivalent resistor network model where the conductors can be represented as edges or facets in a rectilinear Cartesian mesh, then volume-averaged and used as the basis for a DC solution (Yang et al., 2016). Over an unstructured and geometrically-conforming tetrahedral mesh, Weiss (2017) introduced the hierarchical finite element method (Hi-FEM) which, like Yang et al. (2016) uses edge- and facet-based conductivities to account for thin, strong conductors, but avoids its troublesome volume

averaging and restrictive geometry. Regardless of these extensive efforts in the past decades, the complex geometries, the spatial variability, the number of infrastructures and their interactions in geoelectric models still impose high computational loads for 3D simulations and leave most of the existing numerical approaches as problem specific.

In this paper we present case studies from three different subsurface monitoring scenarios, each with variable degrees of infrastructure complexity requiring explicit incorporation in their corresponding geoelectric models. We show how the infrastructure signature is present – in some cases dominant - in the field data and how increasing levels of complexity leads to cumulative effect requiring full field-scale geoelectric modeling.

Case Study #1. CO_2 sequestration at the Containment and Monitoring Institute, Calgary, AB

Proof of concept for the electromagnetic response of a casing defect in a vertical well is relatively straightforward with any number of azimuthally symmetric modeling codes (e.g. Heagy and Oldenburg, 2019a,b) and has recently been addressed in full 3D using finite element (Um et al., 2020; Beskardes et al., 2021). In this section, we further validate the method using field data. Our field-data validation approach is straightforward. Using a surface electric dipole source, we energize two adjacent and intact steel-cased wells having different lengths (i.e., depths) and measure radial surface electric field profiles. Because the length and the properties of the cased wells are known, we can compare the profiles with 3D numerical solutions and cross-validate the concept.

We perform the experiment (Wilt et al., 2020) at the Containment and Monitoring Institute (CaMI) site located in southern Alberta, Canada (Lawton et al., 2017). The CaMI site is a field research station where various existing and experimental geophysical techniques are tested and evaluated for monitoring CO_2 plumes at a relatively shallow depth (**Figure 2**). At the site there are three colinear well heads marking the location of three, corresponding, vertical wells. The central well is an injection well and 550m deep. One observation well (OBS1) is steel-cased and 350m deep. The other observation well (OBS2) is partially steel-cased up to 58m which below the well is fiberglass-cased. In order to demonstrate the concept that a broken steel-cased well produces larger characteristic surface electric fields than expected, we energize the well heads of the two observation wells using a 1 A 5Hz electric bipole source. As shown in **Figure 2**, the return electrode of the electric source is grounded about 500m away from the well head. Voltage measurements are collected along a line of electrodes with 10 m spacing and parallel to the three well heads, offset by a few meters to avoid interfering with well operations and plumbing. Electric field component in the direction of the profile is estimated by taking differences in adjacent electrode voltages and dividing by their (10 m) separation distance. Assuming Gaussian noise overprinting, the electric fields are measured 100 times and averaged for a resultant 10x improvement in signal to noise ratio,

Figure 3 shows the electric field profiles measured for OBS1 and OBS2. The "peak" electric field amplitude for OBS2 is greater than that for OBS1, a finding which is consistent with the relatively high current density supported by the shorter OBS2 well. This is consistent with numerical results although we point out that accurate peak amplitudes are extremely difficult to measure owing to their high spatial gradient and the fact that they are *derived* from discrete voltage differences between adjacent electrode pairs deployed on the ground. Also, the profile for OBS1 is less symmetric compared to that for OBS2 because the surface electric dipole source connected to OBS1 is oblique to the receiver profile. Some data points are deviated from the main profile curves at the same locations of the two profiles due to the effects of steel infrastructure buried in the CAMI site. Evident in these data is the sharp and unmistakable "spike" in electric field strength due to adjacent, passively-coupled injection and monitoring wells.

To quantitatively validate our field experiments, we compare our measurements to 3D numerical solutions. The dominantly layered geology at the CaMI site allows us to easily construct the background resistivity model from borehole resistivity logging data. Using 3D finite-element-based EM modeling algorithm (Um et al., 2020) and well completion diagrams supplied by CaMI, we simulate EM responses to the observation wells. The algorithm uses an internal boundary condition for modeling the steel-cased wells and simulates their EM responses at a small fraction of the cost typically required for full discretization of thin wall casing surrounding a hollow interior. As shown in **Figure 3**, the numerical solutions agree with the field measurements very well. This field experiment and subsequent numerical modeling study confirm that the surface radial electric-field measurements are sensitive to different casing depths, implying that the surface measurements can be used for mapping a discontinuity (i.e., breakage) in a steel-cased well without costly and time-consuming well intervention.

Case Study #2. Casing Integrity Monitoring at Salt Flats oilfield, East Central TX

The electrical anomalies due to infrastructure altering the EM measurements cannot be predicted without modeling. Here, we present a case history from Beskardes et al. (2021) to show how the incorporation of nearby infrastructure into modeling affects the resulting synthetic EM responses. The analysis involves the comparison of the measured electric field data with the synthetic responses obtained from the well models with different degrees and depths of well damage to assess the health of the well (Wilt, 2016; MacLennan et al., 2018; Wilt et al., 2018, 2019, 2020). Due to the sensitivity of the surface EM responses to the changes in geometric and physical properties of steel-cased wells, the analysis not only has potential to detect but also to provide information regarding the rough location of well damage (Beskardes et al., 2021).

As background, GroundMetrics performed a series of casing integrity surveys in February 2018 to evaluate the feasibility of top-casing EM excitation described above at the CaMI site for the problem of non-invasive casing-integrity evaluation at the Salt Flat oil field in Caldwell County, Texas **(Figure 4**). Average well depths in the area ranged from 750m to 850m, which are relatively shallow depths compared to many oil fields and ideal for our study. The specific site discussed here consisted of two wells, Well 4E and Well 1M, located approximately 500m from each other. Well 4E was suspected to have a shallow break in the casing; the owner guessed that it occurred within the top 30 m of the well but did not know exactly. Therefore, the purpose of the field survey was to evaluate the well by examining electric field data collected non-invasively along Earth's surface. Two vertical midcontinent oil wells and a pipeline along with some unmapped power lines are present in the oil field. One of the wells (4E) is damaged at shallow depths as indicated by the camera logs and suggested by the initial analysis with the 3D EM modeling (Wilt et al., 2019). The damaged and intact wells extend 823 m and 837 m in depth and have the conductivity of the steel $\sim 5.5 \times 10^6$ S/m. Both wells have an outer diameter of ~ 0.14 m and a wall thickness of $\sim 9.17 \times 10^{-3}$ m, which corresponds to an area-conductivity product of $\sim 20.7 \times 10^3$ $S \cdot m$. On the other hand, the properties of the pipeline crossing the survey line are not known except its rough location and depth (3 – 4 m). The electric field data was measured along two, roughly NE-SW parallel profiles at low frequencies (0.1, 1 and 10 Hz) by using the top-casing method (Wilt, 2016) where the damaged steel well (4E) was energized at the well head and a return electrode was located at ~ 825 m away for this experiment.

We can compare two aspects from this survey design: first, the measurements from Well 1M to the northeast with the measurements from Well 1M to the southwest; and second, comparing the measurements from Well 1M and from Well 4E. If the former shows similar profiles, then we can assume that the earth is relatively layered and horizontal across the north and south regions in this area, implying that differences between the profiles from the separate wells are due to differences in the wells themselves and not local geology. An initial 1D resistivity model was created from a combination of

resistivity logs from the two wells and a resistivity log from a nearby shallow water well, used to establish the near-surface resistivity values. Well casing properties, including length, thickness, and radius, were provided by well profile logs.

Figure 5 compares the measured data at 1 Hz from of the southern profile through (in-tact) Well 1M with the synthetic profiles using the SimPEG 3D finite volume forward modeling code with a cylindrical mesh (Heagy and Oldenburg, 2019b). This allowed us to model the source current, casing, surface wire and return electrode and to generate the electric field responses along our profile for each frequency. The profile data are fit well by the modeling, and deviations from the modeled data are in areas with known anomalous features, such as pipelines, roads, and power lines. This gives us confidence that the geology is likely to be relatively uniform across the survey area.

Although these data were obtained in the frequency domain, the operational frequencies 0.1 to 10 Hz are indeed low and the success of "static divergence corrections" as brutally effective preconditioners to the full EM induction problem (Smith, 1996) suggests that in some cases a DC interpretation may be sufficient. Here we exercise that assumption with the computationally efficient and flexible Hi-FEM finite element code (Weiss, 2017) which gains its advantage by collapsing thin conductors (like the well casing) to an infinitesimally thin, but finite, conducting filament. At field scales on the order square kilometers, this is often an admissible neglect of fine-scale detail.

To illustrate, we represented both the wells and the pipeline as a sequence of connected edges along tetrahedra within a $10 \times 10 \times 5$ km computation domain. As before, with the SimPEG results, background geology was defined as a layered earth model derived from the resistivity logs. Predictions of DC voltages (**Figure 6**) of the damaged well models with and without the pipeline clearly show the strong distortion on the electric potential distribution caused by the presence of the shallow pipeline with large horizontal extent. Further analysis of particular, casing-defect models such as breaks and corroded patches (Beskardes et al., 2021) suggests that the northern profile, through damaged Well 4E, electric field is best fit by a model with multiple shallow corroded zones over the depth range 10-230 m, consistent with downhole camera observations. This model replicates the comparatively higher amplitude response over an alternative model where damage is absent (**Figure 7**), while also co-locating the damage at a verifiable location. As an aside, it is interesting to note that both in the DC and the full, frequency-domain cases, similar data fits were achieved with a single-defect model (results not shown here) where the damage was isolated to 200 m, far below the region detected by direct observation.

While the analysis confirms the severe condition of the well integrity, it would not be possible to examine the amplitude change in the electric field without incorporating the nearby infrastructure into the modeling since the degree of distortion caused by the infrastructure on the field data would not be known. In this survey, the profiles indicated that the impact of the pipeline is local due to its remote location. On the other hand, these modeling results suggest that the nearby infrastructure may have a more dramatic impact depending on the location, the geometric and electrical properties, the interaction to the other infrastructure and the relative location to survey line and source locations.

Case Study #3. Kern River CA, a Century of Production

As a final example, we embrace the full complexity of the most densely developed oilfield in California, the Kern River, where over 100 years of production has resulted in a tangled tapestry of production pipelines, cased wells and surface pipelines. It is, indeed, a nightmare scenario for electromagnetic prospecting, although it's long been recognized that the dense well-spacing could be exploited for high-resolution cross-well interrogation of both the geology and fluid migration (Wilt and Alumbaugh, 2003).

Here, we expand upon the well-to-well geoelectric model and consider the full richness of the production environment and effect that infrastructure "clutter" has on its geophysical response.

To do so, a 0.7 km^2 patch of the Kern River region was chosen at random and digitized based on features evident in the satellite imagery **(Figure 8)**. In this region 121 well heads were identified, along with 5 surface tanks and roughly 2 km of production pipeline. Assuming an average well depth of 300 m (Wilt and Alumbaugh, 2003), this results in approximately 36 km of steel. Traditional volume-based discretization schemes require on the order of a few million elements per kilometer for discretized pipe, which renders simulation of such scenarios only tenable on the largest of today's supercomputers. To make the calculation tractable for real-time analysis and practical geophysicists, we instead rely on the edge/facet/volume hierarchy of the Hi-FEM method for DC analysis (Weiss, 2017) which collapses pipes to filamentary sequences of connected (finite conductivity) edges with node spacings as great as 10 m. Hence, this 36 km of steel comes at a modest sum to the Hi-FEM modeling universe of only 3600 nodes.

Discretization of 1.2 × 1.2 km domain (the area in Figure 8, buffered by a homogeneous Earth on the sides) that extends 500 m into the ground and into the air was done here with Sandia's CUBIT meshing software (cubit.sandia.gov) which utilizes an advancing front method for tetrahedra and triangle construction. Total mesh size is roughly 2.86M elements over 486k nodes. Hi-FEM uses a Jacobi-preconditioned conjugate gradient iterative solver, which in this case yields results between 3 and 8 minutes on a Mac Pro workstation for a relative residual reduction of 10^{-12}. Although a single mesh was constructed, consideration of infrastructure effects was achieved by simply endowing the relevant edges/facets with non-zero conductances where appropriate. For completeness of the model description, the surface pipelines and well casing were assigned a conductivity-area product of 1×10^4 S·m, tanks a conductance of 1×10^4 S and ground conductivity 0.3 S/m.

We start by asking the simple question: What happens when the top of a single well is energized in such a complex environment? Starting with the least complicated case where all the infrastructure is neglected, we reaffirm the presence of azimuthal symmetry around the energized well (**Figure 9, left**), noting that although the source is a single electrode at the well head, the high casing conductivity results in an effectively "extended" electrode nearly 300m deep. When the remaining wells in the region are then introduced (**Figure 9, center**) we find that the mutual well-to-well galvanic coupling through the weakly conducting Earth results in an overall reduction in the voltage measured over Earth's surface. Clearly, full accounting for all the wells in the region is required to get the amount of reduction right. Also evident is the presence of near-field distortion in the voltage values at every well head. When the tanks and surface pipeline are introduced (**Figure 9, right**), the effect is even more extreme with widespread distortion of voltages due to currents carried by the pipeline. The effect of the full 3D heterogeneity is to reconfigure the radial decay of electric potential from that of the energized well, introducing both scatter and changes in the decay rate, with errors for assuming otherwise greater than 10% at distances as far as several hundred meters (**Figure 10**).

Summary and Conclusions

We have shown through both field examples and simulation results the effect that the presence of metallic artifacts and infrastructure can have on electromagnetic surveys in developed areas. It's long been recognized that this was a problem; we are not the first to point it out. However, we show here some of the latest tools to quantify the effect for realistic survey scenarios and that to proceed unarmed with such tools is to proceed at one's peril. It's helpful, we think, to consider infrastructure effects as having both opportunities for characterization – as in the well casing integrity modeling – and requisite model details for geologic characterization. Both lines of inquiry result in similar modeling and interpretation challenges. Several numerical tools are now in practice (e.g. SimPEG, Hi-FEM) providing the desk-top

geophysicist with real-time analysis strategies that avoid the extreme computational burden of traditional 3D discretization methods. With time and experience, we anticipate that such tools will accelerate the growth of the geophysicist's intuition when presented with data from culturally overprinted areas, and form the basis for novel inversion algorithms and machine-learning datasets for quantitative interpretation.

Data and materials availability

The CaMI data set is available and can be obtained by contacting Evan Um, esum@lbl.gov.

Acknowledgments

The GroundMetrics field work was supported by the US Department of Energy, Office of Science, under Award Number DE-SC0015166. The CaMI work was supported by the U.S. Department of Energy, Office of Energy Efficiency and Renewable Energy, Office of Technology Development, Geothermal Technologies Program and Office of Fossil Energy under contract number DE-AC02-05CH11231. The authors would like to thank multiple colleagues at GroundMetrics who helped to produce these results and the LBNL Geophysical Measurement facility**.** Kern River analysis and development of Hi-FEM hierarchical finite element modeling software was made possible through Sandia National Laboratories LDRD program.

Sandia National Laboratories is a multimission laboratory managed and operated by National Technology and Engineering Solutions of Sandia, LLC., a wholly owned subsidiary of Honeywell International, Inc., for the U.S. Department of Energy's National Nuclear Security Administration under contract DE-NA-0003525.

References

Beskardes, G.D., C.J. Weiss, E. Um, M. Wilt, and K. MacLennan, 2021, The effects of well damage and completion designs on geoelectrical responses in mature wellbore environments: Geophysics, **86**, no. 6, E355–E366, doi: 10.1190/geo2020-0702.1.

Commer, M., G. M. Hoversten, and E. S. Um, 2015, Transient-electromagnetic finite-difference time-domain earth modeling over steel infrastructure: Geophysics, **80**, no. 2, E147–E162, doi: 10.1190/geo2014-0324.1.

Cuevas, N. H., and M. Pezzoli, 2018, On the effect of the metal casing in surface-borehole electromagnetic methods: Geophysics, **83**, no. 3, E173– E187, doi: 10.1190/geo2017-0055.1.

Fitterman, D. V., F. C. Frischknecht, A. T. Mazzella, and W. L. Anderson, 1990, Example of transient electromagnetic soundings in the presence of oil field pipes: Geotechnical and Environmental Geophysics, **2**, 79–88.

Haber, E., C. Schwarzbach, and R. Shekhtman, 2016. Modeling electromagnetic fields in the presence of casing: SEG Tech. Progr. Expand. Abstr 2016, 959–964, doi:10.1190/segam2016-13965568.1.

Heagy, L. J., and D. W. Oldenburg, 2019a, Direct current resistivity with steel-cased wells: Geophysical Journal International, **219**, 1–26, doi: 10.1093/gji/ggz281.

Heagy, L.J. and D.W. Oldenburg. 2019b. Modeling electromagnetics on cylindrical meshes with applications to steel-cased wells. *Computers and Geosciences* 125: 115-30. http://dx.doi.org/10.1016/j.cageo.2018.11.010.

Heagy, L.J., Cockett, R., Kang, S., Rosenkjaer, G.K., and D.W. Oldenburg. 2017. A framework for simulation and inversion in electromagnetics. *Computers and Geosciences* 107: 1-19. http://dx.doi.org/10.1016/j.cageo.2017.06.018.

Holladay, J.S. and G.F. West, 1984, Effect of well casings on surface electrical surveys. Geophysics, **49**, no. 2, 177–188. doi:10.1190/1.1441649.

Kohnke, C., L. Liu, R. Streich, and A. Swidinsky, 2017, A method of mo- ments approach to model the electromagnetic response of multiple steel casings in a layered earth: Geophysics, **83**, no. 2, WB81–WB96, doi: 10 .1190/geo2017-0303.1.

Lawton, D., K. Osadetz, and A. Amin Saeedfar, 2017, CCS monitoring technology innovation at the CaMI field research station, Alberta, Canada: SEG/AEG Research Workshop.

MacLennan, K., Nieuwenhuis, G., Wilt, M., Um, E., and Pendleton, J. M., 2018, Evaluating Well Casing Integrity with Non-Invasive Electromagnetic Methods, SPE Annual Technical Conference and Exhibition, Dallas, Texas, USA, September 2018. https://doi.org/10.2118/191762-MS

Orujov, Gurban, E. Anderson, R. Streich, and A. Swidinsky, 2020, On the electromagnetic response of complex pipeline infrastructure: Geophysics, **85**, no. 6 (2020): E241–E251.

Patzer, C., K. Tietze, and O. Ritter, 2017, Steel-cased wells in 3-D controlled source EM modelling: Geophysical Journal International, **209**, 813–826, doi: 10.1093/gji/ggx049.

Ronczka, M., C. Rücker, and T. Günther, 2015, Numerical study of long-electrode electric resistivity tomography — Accuracy, sensitivity, and resolution: Geophysics, **80**, no. 6, E317–E328, doi: 10.1190/geo2014-0551.1.

Rucker,D.F., M.H. Loke, M.T. Levitt, and G.E. Noonan, 2010, Electrical-resistivity characterization of an industrial site using long electrodes: Geophysics, 75, no. 4, WA95.

Rücker, C., and T. Günther, 2011, The simulation of finite ERT electrodes using the complete electrode model: Geophysics, **76**, no. 4, F227–F238, doi: 10.1190/1.3581356.

Smith, T.J., 1996, Conservative modeling of 3-D electromagnetic fields, Part II: Bi-conjugate gradient solution and a solver. Geophysics, **61**, 1319-24, doi: 10.1190/1.1444055.

Swidinsky, A., R.N. Edwards, and M. Jegen, 2013, The marine controlled source electromagnetic response of a steel borehole casing applications for the NEPTUNE Canada gas hydrate observatory: Geophys. Prospect, **61**, no. 4, 842–856.

Tang, W., Y. Li, A. Swidinsky, and J. Liu, 2015, Three-dimensional con- trolled-source electromagnetic modelling with a well casing as a grounded source: A hybrid method of moments and finite element scheme: Geophysical Prospecting, **63**, 1491–1507, doi: 10.1111/1365-2478.12330.

Um, E. S., M. Commer, G. A. Newman, and G. M. Hoversten, 2015, Finite element modelling of transient electromagnetic fields near steel-cased wells: Geophysical Journal International, **202**, 901–913, doi: 10.1093/ gji/ggv193.

Qian, W., and D.E. Boerner, 1995, Electromagnetic modelling of buried line conductors using an integral equation: Geophysical Journal International, **121**, no. 1, 203–214.

Um, E. S., and Wilt, M. J., 2018, Top-Casing Electric Source Method for Assessing Wellbore Integrity: Electromagnetic Approach, SEG International Exposition and Annual Meeting, Anaheim, California, USA, https://doi.org/10.1190/segam2018-W10-02.1.

Um, E.S., Kim, J. and Wilt, M., 2020. 3D borehole-to-surface and surface electromagnetic modeling and inversion in the presence of steel infrastructure. Geophysics, 85(5), pp.E139-E15.

Wait, J.R., 1972, The effect of a buried conductor on the subsurface fields for line source excitation: Radio Science **7**, no. 5, 587–591.

Wait, J.R., 1983. Resistivity Response of a Homogeneous Earth with a Contained Vertical Conductor. pp. 1.

Wait, J.R. and D.A. Hill, 1973, Excitation of a homogeneous conductive cylinder of finite length by a prescribed axial current distribution: Radio Sci., **8**, no. 12, 1169–1176.

Wang, M., F. J. Dickin, and R. Mann, 1999, Electrical resistance tomographic sensing systems for industrial applications: Chemical Engineering Communications, **175**, 49–70, doi: 10.1080/00986449908912139.

Weiss, C. J., 2017, Finite-element analysis for model parameters distributed on a hierarchy of geometric simplices: Geophysics, **82**, no. 4, E155–E167, doi: 10.1190/geo2017-0058.1.

Wilt M. J. and Alumbaugh, D. L., 2003, Oil field reservoir characterization and monitoring using electromagnetic geophysical techniques, Journal of Petroleum Science and Engineering, **39**, 85-97.

Wilt, M., 2016, Wellbore integrity mapping using well-casing electrodes and surface based electrical fields: Final Report for SBIR phase 1 Grant DE- SC0015166.

Wilt, M., Nieuwenhuis, G., MacLennan, K., and Um, E., 2018, Casing-integrity mapping using top-casing electrodes and surface based EM fields, SEG Technical Program Expanded Abstracts, p 858-862.

Wilt, M., E. Um, K. MacLennan, C. J. Weiss, and G. D. Beskardes, 2019, Case histories applying top-casing electrodes and surface-based EM fields for well integrity mapping: 89th Annual International Meeting, SEG, Expanded Abstracts, 1120–1124, doi: 10.1190/segam2019-3216490.1.

Wilt, M. J., E. S. Um, E. Nichols, C. J. Weiss, G. Nieuwenhuis, and K. MacLennan, 2020, Casing integrity mapping using top-casing electrodes and surface-based electromagnetic fields: Geophysics, 85, no. 1, E1–E13, doi: https://doi.org/10.1190/geo2018-0692.1.

Yang, D., D. Oldenburg, and L. Heagy, 2016, 3D DC resistivity modeling of steel casing for reservoir monitoring using equivalent resistor network: 86th Annual International Meeting, SEG, Expanded Abstracts, 932– 936, doi: 10.1190/segam2016-13868475.1.

Zhang, J., R. L. Mackie, and T. R. Madden, 1995, 3-D resistivity forward modeling and inversion using conjugate gradients: Geophysics, **60**, 1313– 1325, doi: 10.1190/1.1443868.

Figure 1. Mature oilfields, such as that shown here near Bakersfield CA, are typically characterized by a rich assemblage of cultural artifacts such as pipelines, buildings, powerlines, etc., reflecting decades of coordinated and evolving reservoir production.

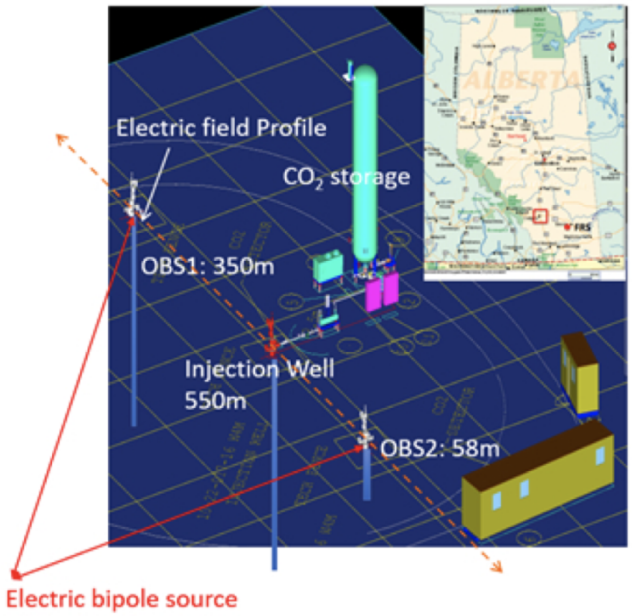

Figure 2. Rendering of the CaMI field research station, a site for CO2 sequestration, located about 200 km east of Calgary, Alberta. Like the oilfield example, sites such as these where long-term continuous monitoring of subsurface processes are challenged by the effects of infrastructure overprinting on geophysical data.

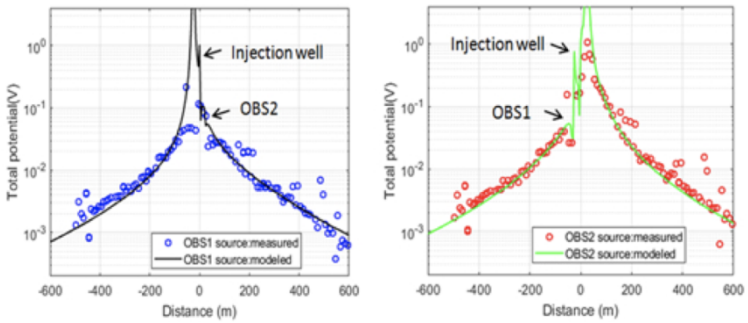

Figure 3. Observed (symbols) and modeled in-line electric field at the CaMI site (Figure 2) showing abrupt anomalies due to the presence of adjacent wells.

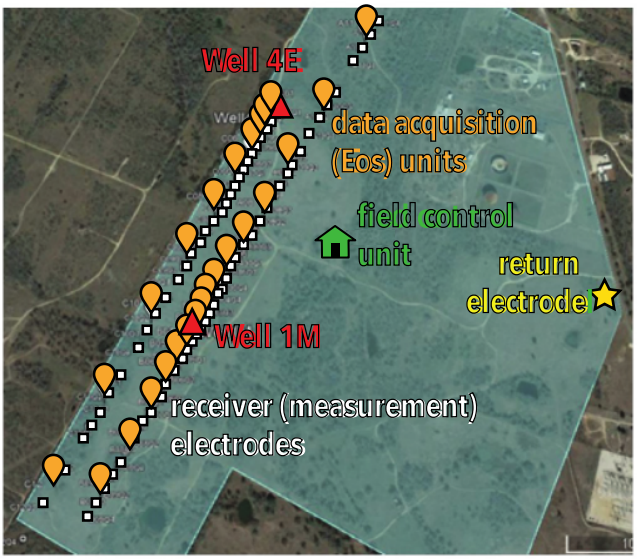

Figure 4. Satellite photo of the Salt Flats (TX) oilfield with well sources (red triangles), data acquisition system (Eos) locations (orange markers) and receiver locations (white squares). The shaded area represents property line boundaries. The field control unit is denoted by the green house and the return electrode to the east is the yellow star.

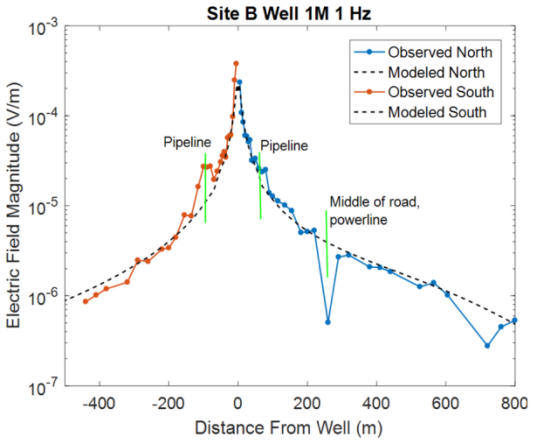

Figure 5. Modeled and measured in-line electric field along the profile in Figure 4 intersecting well 1M (bottom line). Notice the generally exponential falloff in intensity for a layered Earth, but superposed with mild scatter due to subtle heterogeneity that is overshadowed by more prominent anthropogenic signatures.

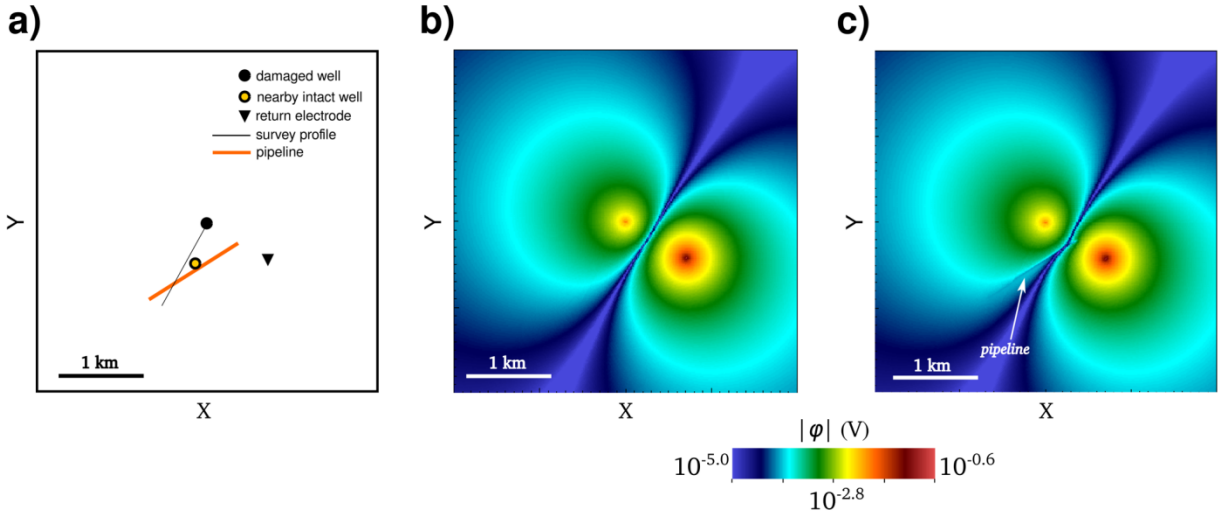

Figure 6. Direct current electrostatic survey simulation over a simplified, mature oilfield (Figure 4) with only two wells and a single oblique pipeline nearby (left). Predicted potentials on Earth's surface show a clear and measurable distinction between instances where the pipeline is absent (center) and present (right).

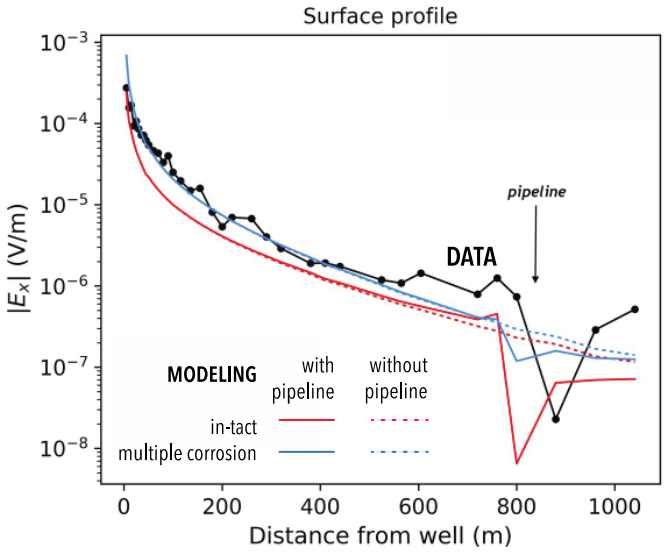

Figure 7. Observed and predicted horizontal DC electric field along upper profile in Figure 4, through well 4E where, again, the surface pipeline yields an anomaly whose amplitude far exceeds the noise. Simulation results where both casing corrosion and the pipeline are present (solid blue) generally recover the character of the observed data.

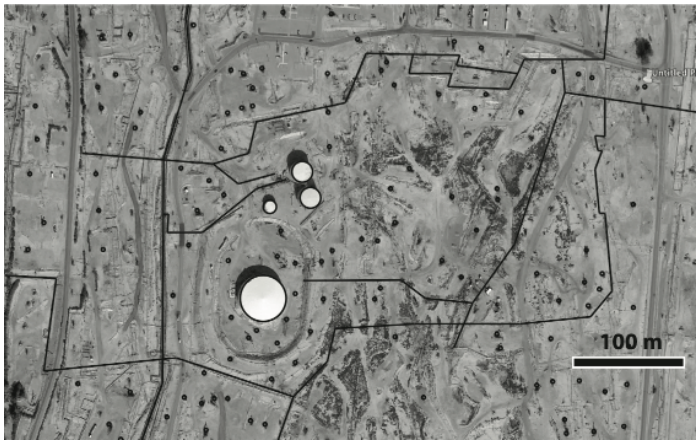

Figure 8. Satellite photograph of a representative patch of the Kern River oilfield near Bakersfield CA showing 121 vertical wells at depths 250-300 m, 4 storage tanks and roughly 2 km of surface pipeline.

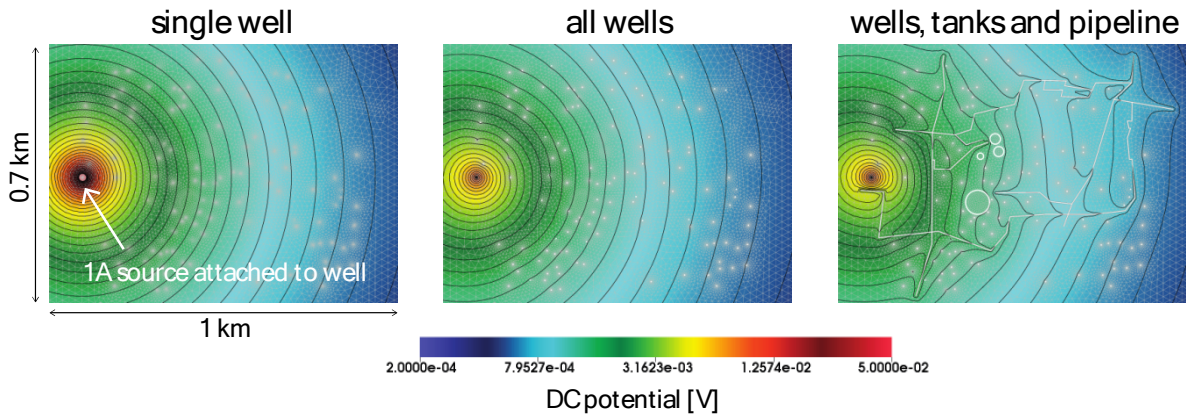

Figure 9. Simulation results for the Kern River site (Figure 8) for the case of a 1 A direct current source attached to a single, cased well, alone (left), in the presence of the remaining 120 cased wells (center), and in the presence of all wells, tanks and surface pipelines (right).

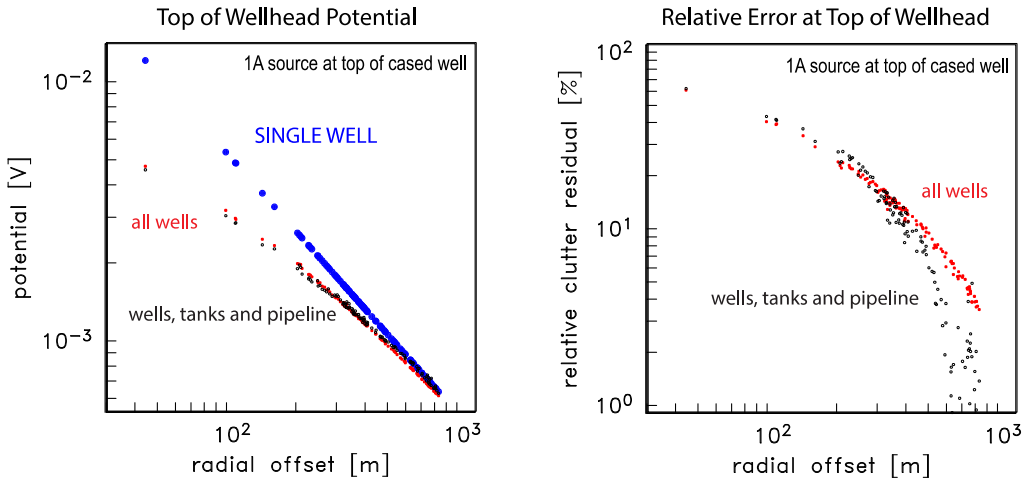

Figure 10. Top casing electrostatic potentials plotted a function distance from the source well for the three scenarios shown in Figure 9 (left). Note the breakdown in radial symmetry (increase in scatter) as more infrastructure is considered. Relative error with respect to the single-well results (right) show that neglect of complete infrastructure accounting can result in errors in excess of 10% at distances as far away as 0.5 km.